Magnetic permeability for exchange-spring magnets: Application to Fe/Sm-Co

R. J. Astalos and R. E. Camley

Department of Physics, University of Colorado at Colorado Springs, Colorado Springs, Colorado 80933-7150

(Received 14 October 1997; revised manuscript received 15 December 1997)

We investigate the properties of the dynamic permeability for a layered structure composed of a ferromagnet with low anisotropy coupled to a ferromagnet with high anisotropy. The permeability of a structure with a small number of layers (<200) can be directly calculated numerically with few approximations in the long-wavelength limit. For larger structures we obtain analytic forms for the permeability which are appropriate in the weak-coupling limit. Our results give the resonance frequency as a function of the thickness of the two materials, the interface and bulk exchange fields, and the anisotropy in each material. We find that significant shifts in the resonance frequency, on the order of 40 GHz, can be obtained with only a small reduction in the strength of the resonance. This can be important for high-frequency signal-processing devices, and we calculate the properties of a filter based on a Fe/Sm-Co material. [S0163-1829(98)03037-9]

I. INTRODUCTION

Recently there has been increasing interest in exchange-spring systems which are mixtures of hard and soft magnetic materials.[1–4] These materials typically combine the high anisotropy found in some rare-earth dominated permanent magnets with the larger magnetic moment found in transition-metal ferromagnets. These materials have a number of uses, including exchange biasing applications and as permanent magnets.

A recent paper[1] studied exchange-spring bilayers composed of magnetically hard Sm-Co(1100) and a transition metal ferromagnet. In addition to static measurements such as that of a hysteresis curve, this paper also presented information on dynamic spin wave modes through Brillouin light scattering. The analysis of the spin wave frequencies was limited but interesting. It was shown that there was an effective exchange field, H_{ex}, acting on the transition metal ferromagnet due to the coupling with the high-anisotropy Sm-Co. When this exchange field was added to the applied field, conventional spin wave theory gives the correct value for the lowest spin wave frequency of the system. This result is quite encouraging for applications in high frequency signal processing, since it shows that substantial frequency shifts may be obtained by coupling Fe or Co films to high anisotropy materials. For example, with the applied field set to zero, one normally expects the spin wave frequency of a thin Fe or Co film to also be close to zero. However, due to the coupling and the high anisotropy in Sm-Co, the spin wave frequency is shifted up by about 20 GHz.

There are a number of improvements, however, which should be made to such a calculation. Normally the electromagnetic response of a material is characterized by the frequency dependent permeability tensor, rather than just by a single frequency. This tensor provides information on the ellipticity of the magnetic precession and on the strength of the dynamic response of the system to small driving fields as well as information on the excitation frequencies. The permeability tensor, or equivalently the susceptibility, is fundamental for calculations of Brillouin light scattering intensities and the response of the structure in ferromagnetic

resonance experiments. Such information is also vital to characterizing and employing the exchange-spring materials, and we illustrate this with a calculation of the properties of a high frequency magnetic filter based on the exchange spring permeability derived here.

In this paper we present a microscopic calculation for the permeability tensor of an exchange-spring system. This calculation gives results based on the microscopic parameters of the structure: the number of layers of the hard and soft materials, the exchange and anisotropy constants in each material, and the interface exchange couplings. We can thus make numerical predictions for the resonance frequencies for Fe/Sm-Co structures as a function of the thickness of the different films.

The initial calculations described above are outlined analytically, but must be completed numerically. It is, however, useful to have analytic forms for the permeability tensor, at least in some limits. In the weak to moderate interface coupling limit the structure can be approximated by two blocks of spins, one for the transition metal ferromagnet and one for the hard ferromagnet. These blocks of spins are coupled by an effective interfacial exchange which depends on the number of layers of each material. In this limit we obtain a simplified set of equations which can be solved analytically. When the analytic results are compared to the numerical ones, we find that they are in very good agreement for weak interfacial coupling, and that even for moderate interfacial coupling the analytic solutions provide a reasonable estimate.

Finally, we illustrate the use of the permeability tensor in an example calculation for the properties of a high frequency filter based on an exchange-spring material as the active medium. We find that coupling of Fe to Sm-Co can raise operating frequencies significantly without substantially reducing the performance of the filter.

II. MICROSCOPIC DEVELOPMENT OF PERMEABILITY TENSOR

We can set up the geometry quite generally on a layer by layer basis. As is shown in Fig. 1 the equilibrium positions of
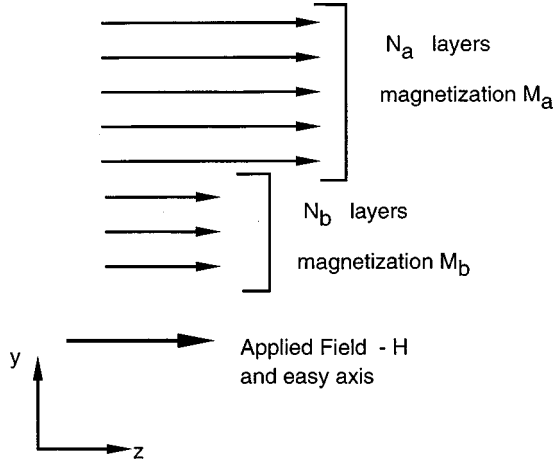
FIG. 1. Illustration of the geometry of the structure. The applied field is along the z axis and the y axis is perpendicular to the layers.

the spins in each layer are assumed to lie in the z direction. The instantaneous direction will, of course, vary from this position. There is a constant applied field H also in the z direction and this is also the easy axis for both materials. There are N_a layers of the soft ferromagnet and N_b layers of the hard Sm-Co. Throughout the paper we will refer to particular layer structures as N_a/N_b meaning the (number of Fe layers)/(number of Sm-Co layers). While we show just a bilayer system here, a superlattice can be easily constructed by imposing periodic boundary conditions in the y direction.

The total energy density of the system may be written[1]

$$E = -\sum_{i=1}^{N-1}\left(\frac{A_{i,i+1}}{d^2}\right)\mathbf{a}^{(i)}\cdot\mathbf{a}^{(i+1)} - \sum_{i=1}^{N}K_i(a_z^{(i)})^2$$
$$-\sum_{i=1}^{N}(\mathbf{H}+\mathbf{h}^{(i)})\cdot\mathbf{a}^{(i)}M^{(i)}. \quad (1)$$

Here $\mathbf{M}^{(i)}$ is the magnetization vector in layer i, K_i the anisotropy constant for layer i, and $A_{i,i+1}$ is the exchange coupling constant between layers i and $i+1$. The quantity $\mathbf{h}^{(i)}$ is a small fluctuating magnetic field. The total number of layers is $N = N_a + N_b$. The distance between magnetic layers is d. For convenience, we have changed to unitless variables for the magnetization, i.e., $\mathbf{a}^{(i)} = \mathbf{M}^{(i)}/M^{(i)}$. To obtain the permeability tensor, we need to find the response of the magnetization to a small fluctuating driving field $\mathbf{h}^{(i)}$ which can vary from layer to layer. Effective medium methods for dealing with magnetic layered structures have been developed in the past.[5,6] However, these methods depend on the interfacial exchange being weak compared to the exchange within an individual material. This is appropriate for structures such as Fe/Cr/Fe, Fe/Cu/Fe, or Co/Cu/Co where the effective exchange coupling between the Fe films through the nonmagnetic film is only a few percent of the intrafilm exchange coupling.[7-10] However, recent experiments on Sm-Co/transition metal systems show very strong interfacial exchange. Thus we turn to a microscopic method developed recently[11] which does not depend on weak interfacial exchange.

This calculation is done in the long-wavelength limit appropriate to the applications mentioned above—

ferromagnetic resonance, filter applications, and Brillouin light scattering. In this limit the wavelength of the spin waves parallel to the surface is thousands of atoms long and it is a reasonable approximation to neglect intralayer variations in magnetization because the contribution of the exchange and magnetostatic energies is very small. We note that there has been some previous theoretical work[11] comparing calculations which take into account full *interatomic* exchange with calculations in the long wavelength limit which include only *interlayer* exchange. This work showed that in the long wavelength limit the interlayer exchange model worked very well for films under a few hundred Å. In fact the answers produced by the full calculation were less than a few percent different than those which include only interlayer coupling. Of course, in some calculations interatomic exchange can be important, e.g., in the calculation of nucleation fields in exchange-spring systems.[12]

We start with the Bloch equations of motion for the spin system. The equations of motion for layer i are given by

$$\frac{d\mathbf{a}^{(i)}}{dt} = \gamma\mathbf{a}^{(i)}\times(\mathbf{H}_{\text{eff}}+\mathbf{h}^{(i)}). \quad (2)$$

Here γ is the gyromagnetic ratio. $\mathbf{H}_{\text{eff}}$ is the effective field acting on layer (i) produced through the energy density given above through the definition $\mathbf{H}_{\text{eff}} = -\partial E/\partial \mathbf{M}^{(i)} = -(1/M^{(i)})\partial E/\partial\mathbf{a}^{(i)}$. Using this definition and Eq. (1) we may define the following effective fields. The effective exchange field in layer i is given by contributions from the layers both above and below:

$$\mathbf{H}_{\text{ex}}^{(i)} = \left(\frac{A_{i-1,i}}{d^2M^{(i)}}\right)\mathbf{a}^{(i-1)} + \left(\frac{A_{i,i+1}}{d^2M^{(i)}}\right)\mathbf{a}^{(i+1)}$$
$$= H_e^{i-1}\mathbf{a}^{(i-1)} + H_e^{i+1}\mathbf{a}^{(i+1)}. \quad (3)$$

The effective anisotropy field (in the z direction) is given by $H_a^{(i)} = (2K_i/M^{(i)})a_z^{(i)}$.

In this way the equations of motion for an arbitrary layer (i) may be written explicitly. We assume that the driving field $\mathbf{h}$ and the dynamic magnetization vectors $\mathbf{a}$ both have a time dependence of the form $\exp(-i\omega t)$. The equations of motion become

$$\frac{i\omega}{\gamma}a_x^{(i)} + (H_a^{(i)}+H+H_e^{(i-1)}+H_e^{(i+1)})a_y^{(i)}$$
$$-H_e^{(i-1)}a_y^{(i-1)} - H_e^{(i+1)}a_y^{(i+1)} = h_y^{(i)} \quad (4)$$

and

$$\frac{i\omega}{\gamma}a_y^{(i)} - (H_a^{(i)}+H+H_e^{(i-1)}+H_e^{(i+1)})a_x^{(i)}$$
$$+H_e^{(i-1)}a_x^{(i-1)} + H_e^{(i+1)}a_x^{(i+1)} = -h_x^{(i)}. \quad (5)$$

In order to form the susceptibility, we need to connect the average magnetization for the entire structure to the average driving fields. The average magnetization is given by

$$\langle \mathbf{m} \rangle = \frac{1}{N} \sum_{i=1}^{N} \mathbf{a}^{(i)} M^{(i)} \tag{6}$$

and the average driving field is given by

$$\langle \mathbf{h} \rangle = \frac{1}{N} \sum_{i=1}^{N} \mathbf{h}^{(i)}. \tag{7}$$

The set of equations of motion for the N layers provide $2N$ equations connecting the $\mathbf{a}^{(i)}$ to the $\mathbf{h}^{(i)}$. There are, however, additional connections provided by the boundary conditions. In the long wavelength limit, we expect that the tangential components of $\mathbf{h}$ in each layer will be the same, i.e., $h_x^{(1)} = \cdots = h_x^{(i)} = C_x$. Furthermore, the normal components of the $\mathbf{B}$ field must also be continuous. Thus $h_y^{(1)} + 4\pi a_y^{(1)} M^{(1)} \cdots = h_y^{(i)} + 4\pi a_y^{(i)} M^{(i)} = C_y$. The amplitudes C_x and C_y are constants.

The susceptibility χ connecting the average magnetization to the average driving field according to $\langle \mathbf{m} \rangle = \widetilde{\chi} \langle \mathbf{h} \rangle$ can now be determined numerically. The boundary conditions together with the equations of motion provide a total of $3N + 1$ equations connecting the amplitudes $\mathbf{a}^{(i)}$ and $\mathbf{h}^{(i)}$ to the constants C_x and C_y. For a given frequency ω, we choose $C_x = 0$ and $C_y = 1$ and then using a linear equation solver we may solve explicitly for all the $\mathbf{a}^{(i)}$ and $\mathbf{h}^{(i)}$. We can then form the average fields $\langle \mathbf{m} \rangle$ and $\langle \mathbf{h} \rangle$ according to Eqs. (6) and (7). With the choice of C's above $\langle h_x \rangle = 0$ and we may immediately find χ_{yx} and χ_{yy} by $\chi_{xy} = \langle m_x \rangle / \langle h_y \rangle$ and $\chi_{yy} = \langle m_y \rangle / \langle h_y \rangle$. To find the remaining components of the susceptibility tensor we repeat the calculation with $C_x = 1$. This allows us to find χ_{xy} and χ_{yx} by using the relations $\chi_{xx} = (\langle m_x \rangle - \chi_{xy} \langle h_y \rangle) / \langle h_x \rangle$ and $\chi_{yx} = (\langle m_y \rangle - \chi_{yy} \langle h_y \rangle) / \langle h_x \rangle$.

It is important to note that one expects $\chi_{xy} = -\chi_{yx}$. This provides an important check on the solution. From the computed values of χ we then obtain the permeability tensor using the relation $\mu = \mathbf{1} + 4\pi\chi$. Our tensor for the permeability takes the usual form for an anisotropic and gyrotropic material

$$\mu = \begin{pmatrix} \mu_{xx} & \mu_{xy} & 0 \\ \mu_{yx} & \mu_{yy} & 0 \\ 0 & 0 & 1 \end{pmatrix} = \begin{pmatrix} \mu_1 & i\mu_t & 0 \\ -i\mu_t & \mu_2 & 0 \\ 0 & 0 & 1 \end{pmatrix}. \tag{8}$$

In order to include the effects of dissipation, we replace $\omega \rightarrow \omega + i\Gamma$ in our calculations. This makes all the permeability terms complex, but we focus on the real parts of the diagonal elements and the imaginary portion of the off diagonal terms.

We explore the numerical results for the permeability first in the limit when the coupling is zero. The parameters used in the calculation are those given in Ref. 1, i.e., $A_{i,i+1} = 1.2 \times 10^{-6}$ ergs/cm for the Sm-Co, $A_{i,i+1} = 2.8 \times 10^{-6}$ for Fe, $K_i = 5 \times 10^7$ erg/cm^3 for Sm-Co, $K_i = 10^3$ erg/cm^3 for Fe, $M_s = 550$ emu/cm^3 for Sm-Co, and $M_s = 1700$ emu/cm^3 for Fe. The gyromagnetic ratio is taken to be 2.92 GHz/kG, the value appropriate for Fe. We use an applied field of 2 kG and take Γ to be 200 G, a reasonable value for metallic systems.

In Fig. 2 we plot the low frequency permeability for different values of the number of hard and soft magnetic layers. For a pure Fe film, the resonance in the permeability ele-
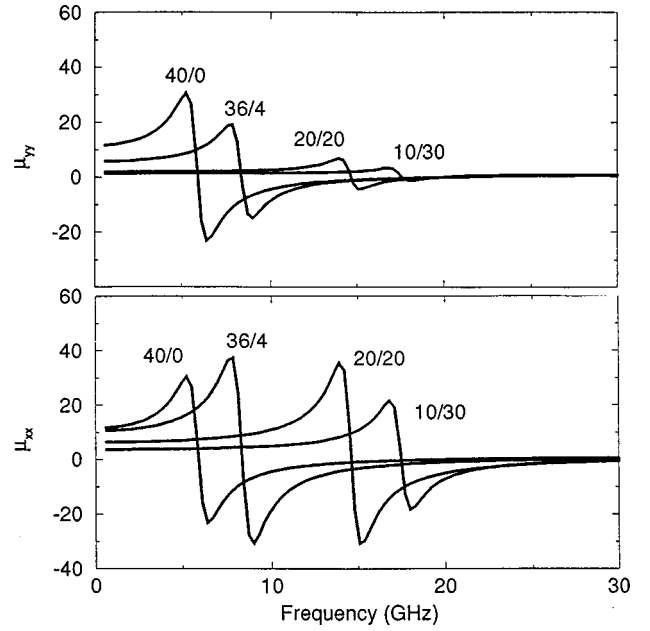

FIG. 2. μ_{yy} and μ_{xx} as a function of frequency for different layerings. The 40/0 notation means 40 layers of Fe and zero layers of Sm-Co. The interface coupling is zero. Note the difference in magnitude between μ_{yy} and μ_{xx}.

ments occurs at the frequency associated with the applied field, γH. For $H = 2$ kG used here, we expect the resonance at 5.84 GHz. We see that even in the absence of exchange coupling, the resonance frequency shifts upward for both μ_{xx} and μ_{yy} as the number of Sm-Co layers is increased. In addition the size of the resonant signature decreases for μ_{yy} but increases (initially) for μ_{xx}. We can obtain a feeling for the anisotropy in precessional motion due to the layering when we compare μ_{yy} to μ_{xx}. In an isotropic material, these are the same. In Fig. 2 however, we see that as the amount of Sm-Co is increased, the permeability becomes more anisotropic.

In Fig. 3 we explore how μ_{yy} and μ_{xx} depend on interface coupling. We examine the results for the 36/4 structure with the interfacial coupling varying from zero to the value found in recent experiments. One feature is immediately obvious. There is a substantial shift in the resonance frequency as the interfacial coupling is increased. In addition, the values for μ_{yy} and μ_{xx} approach each other as the coupling is increased. Thus the coupling has nearly restored the condition $\mu_{yy} = \mu_{xx}$ which is found when there is no layering.

A comment on the shift in the resonance as the interfacial coupling is increased from zero is appropriate. For Fe/Cr/Fe type systems, it is well known that the low frequency excitations for a magnetic bilayer can be classified as "acoustic" or "optic" type modes.[13–16] The acoustic mode essentially has all the spins moving together and as a result is not strongly influenced by interfacial exchange. For that system it is the optic mode, where the spins in the two Fe films are not moving together, which strongly depends on interface exchange.

The situation is quite different in the Fe/Sm-Co structure studied here. The lowest frequency mode is basically the acoustic mode, but it is not shifted from just the exchange interaction alone. In this case the interaction of the Fe spins with the high anisotropy Sm-Co spins has made the spin
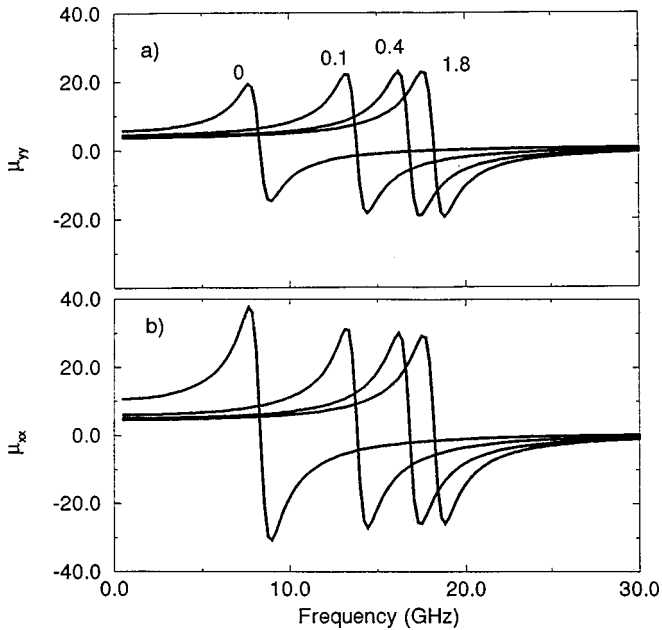
FIG. 3. μ_{yy} and μ_{xx} as a function of frequency for different values of interface coupling. The structure is 36/4 (36 layers of Fe and 4 layers of Sm-Co). The numbers indicate the values for A_I, e.g., a number of 1.8 indicates the full experimental coupling value of $A_I = 1.8 \times 10^{-6}$ ergs/cm. Note the shift in frequency as coupling is increased. Also the difference in magnitude between μ_{yy} and μ_{xx} is reduced as the coupling is increased.

FIG. 4. (a) The Voigt permeability, μ_v, as a function of frequency for different layerings indicated by the numbers. The 40/0 notation means 40 layers of Fe and zero layers of Sm-Co. The interface coupling is zero. (b) μ_v as a function of frequency for different layerings. The interface coupling has its maximum experimental value of $A_I = 1.8 \times 10^{-6}$ ergs/cm.

system much ''stiffer'' and therefore substantially raised the frequency. Thus we have a case of exchange-coupled anisotropies discussed recently in the literature for ferromagnet/antiferromagnet structures.[17]

We note that the parameters used in our calculation are those obtained from static measurements in Ref. 1. When we use the dynamic permeability tensor obtained here in the standard calculation for magnetostatic wave frequencies, we obtain excellent agreement for both the zero field value of the frequency found in Ref. 1 and the field dependence of the frequency. The experimental and theoretical values lie within a few percent of each other.

The shift of the resonance seen in Fig. 2, even in the absence of interfacial coupling, is somewhat misleading. Of course, μ_{yy} and μ_{xx} are only individual components of the permeability tensor and do not represent the general interaction of electromagnetic radiation with the material. A better measure is the Voigt permeability[18] given by $\mu_v = (\mu_1 \mu_2 - \mu_t^2)/\mu_2$.

In Fig. 4(a) we therefore plot the behavior of μ_v as a function of frequency again for structures with different layerings. If there is only Fe, the resonance frequency in the Voigt permeability occurs at the usual value for a thin Fe film given by $\omega_r = \gamma \sqrt{H(H + 4\pi M_a)}$. For the parameters used here this frequency occurs at about 20 GHz. In contrast to the results for μ_{yy}, the resonance frequency in the Voigt permeability does not shift substantially with different layerings in the absence of coupling. The main feature seen here is that the strength of the resonance shrinks as more Sm-Co layers are introduced.

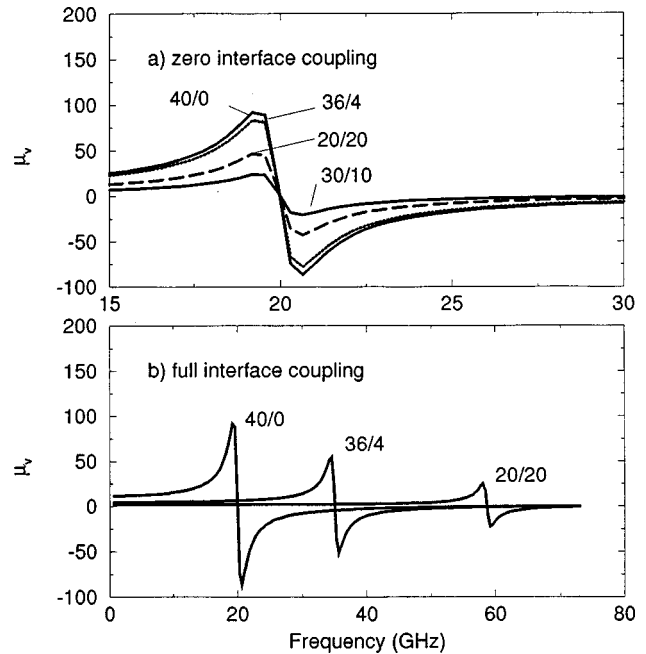Figure 4(b) shows the behavior of the Voigt permeability as a function of frequency when interface exchange is in-

cluded. In contrast to Fig. 4(a) where interfacial exchange is zero, we see in this figure a dramatic upward shift in the resonance position as more Sm-Co layers are introduced into the structure.

A key point of Figs. 2–4 is that as long as the number of Sm-Co layers is rather small, the strength of resonance in the layered structure is not significantly reduced from that of pure Fe. We therefore in Fig. 5 look at the effect of different interface coupling constants for a structure with 4 layers Sm-Co and 36 layers of Fe. A relatively small interface coupling of $A_I = 0.1 \times 10^6$ ergs/cm already shifts the frequency up by about 10 GHz. Using the interface coupling found in Ref. 1 of 1.8×10^6 ergs/cm the frequency for the resonance
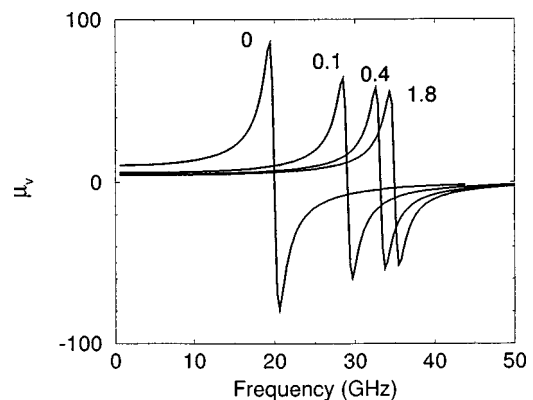

FIG. 5. Effect of interface exchange on μ_v for the 36/4 (36 layers Fe/4 layers Sm-Co) structure. The numbers indicate the values for A_I, e.g., a number of 1.8 indicates the full experimental coupling value of $A_I = 1.8 \times 10^{-6}$ ergs/cm.
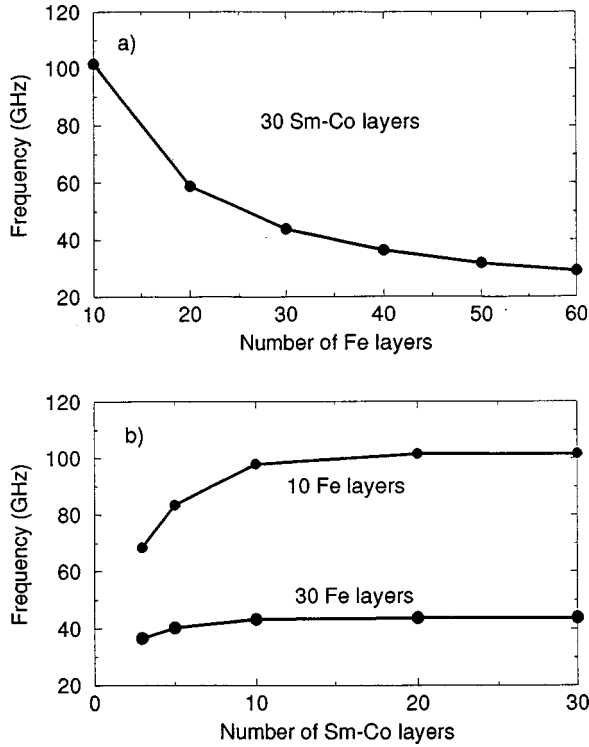
FIG. 6. Influence of layering structure on resonance frequencies of the Voigt permeability. We assume full interfacial coupling of $A_I = 1.8 \times 10^{-6}$ ergs/cm. (a) Frequency as a function of the number of Sm-Co layers for fixed number of Fe layers; (b) frequency as a function of the number of Fe layers for a fixed number of Sm-Co layers.
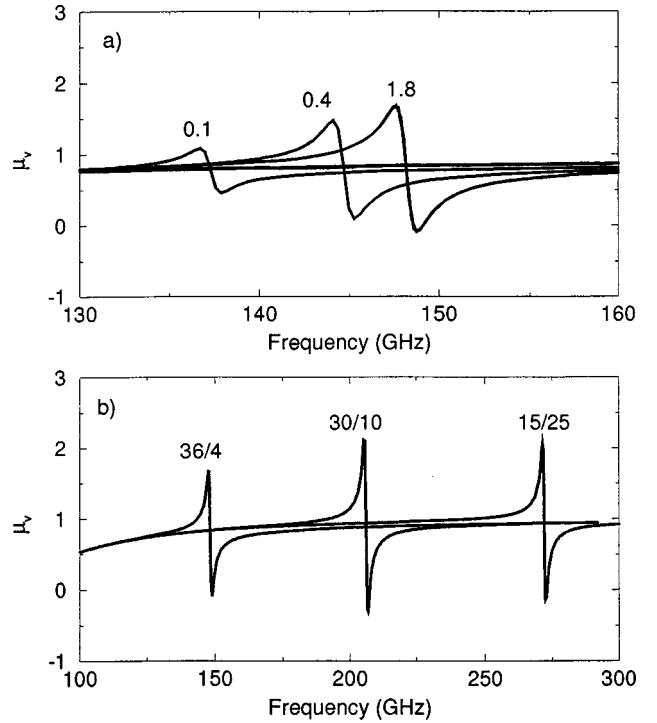

FIG. 7. Examination of high frequency mode resonances in the Voigt permeability: (a) Frequency as a function of interface exchange for 36/4 (36 layers Fe/4 layers Sm-Co) structure. The numbers indicate the interfacial coupling, e.g., 1.8 indicates that $A_I = 1.8 \times 10^{-6}$ ergs/cm. (b) Frequency as a function of layering structure for full interface coupling.

has nearly doubled and the strength of the resonance is only slightly reduced from the pure Fe case.

In Fig. 6 we explore how the frequency depends on the number of layers of one material when the number of layers of the other is held constant. In Fig. 6(a) the number of Sm-Co layers is held constant at 30 and the number of Fe layers is varied. As the number of Fe layers is reduced, the frequency increases rapidly. The shift in the frequency from the infinite thickness value is close to a 1/thickness dependence. The origin for this will be discussed in the next section. In contrast, the dependence of the frequency on the Sm-Co thickness is much weaker. As is seen in Fig. 6(b), the frequency remains essentially constant with Sm-Co thickness for films thicker than 10 layers. As the thickness is reduced below 10 layers, however, the frequency shifts downward.

Using this method we can also explore the higher frequency resonances. In Fig. 7 we show how the second resonance in the structure depends on interface coupling and on layering pattern. Figure 7(a) plots the Voigt permeability as a function of frequency for different interfacial coupling constants. As the coupling is increased, both the frequency and the strength of the resonance increase. The strength of the resonance is significantly reduced compared to the lower frequency one investigated in Figs. 2–6, however, with the strength of this resonance being only about 3% of that for the lower frequency one. Nonetheless, it may be possible to measure and use this resonance. Figure 7(b) again examines the Voigt permeability as a function of frequency, but this

time the interfacial coupling is kept constant and the structure is varied. Clearly, changes in the structure can produce significant changes in the resonance frequency.

III. ANALYTIC RESULTS FOR THE PERMEABILITY IN THE WEAK COUPLING LIMIT

While the calculation in Sec. II will, in principle, find the permeability for any number of layers, it becomes more difficult as the number of layers increases. For example for a typical 500 Å structure, one must find the solution to a set of 751 linear equations. Therefore it is helpful to obtain analytic results when possible. In this section we concentrate on an approximation which dramatically simplifies the calculation allowing analytic forms to be found.

If the coupling between the interfacial layers is weak compared to the coupling within the different materials, then one may essentially treat the system as two blocks of spins with one block representing each material. To find the equations of motion for the two blocks of spins, one adds together all the equations of motion for each component of material A and material B separately. With the assumption that all the spins in material A move rigidly together and that all the spins in material B move rigidly together we then have

$$a_x^{(1)} = a_x^{(2)} = \cdots = a_x^{(N_a)} = a_x \qquad (9)$$

and

$$b_x^{(N_a+1)} = b_x^{(N_a+2)} = \cdots = b_x^{(N_a+N_b)} = b_x \qquad (10)$$

and similar equations hold for the y component. The entire set of $2(N_a+N_b)$ equations of motion for the spin system then reduce to just four equations given by

$$\begin{pmatrix} h_y^a \\ -h_x^a \\ h_y^b \\ -h_x^b \end{pmatrix} = \begin{pmatrix} i\omega/\gamma & H_1 & 0 & -H_{e1} \\ -H_1 & i\omega/\gamma & H_{e1} & 0 \\ 0 & -H_{e2} & i\omega/\gamma & H_2 \\ H_{e2} & 0 & -H_2 & i\omega/\gamma \end{pmatrix} \begin{pmatrix} a_x \\ a_y \\ b_x \\ b_y \end{pmatrix}. \tag{11}$$

In the above we have used $H_1 = H_a^{(a)} + H + H_{e1}$ and the effective exchange field acting on material A is given by $H_{e1} = A_I/d^2 M^{(a)} N_a$ where A_I is the interface coupling constant.

Similarly we have for material B $H_2 = H_a^{(b)} + H + H_{e2}$ where $H_{e2} = A_I/d^2 M^{(b)} N_b$.

We see that the exchange coupling term H_{e1} for the effective field acting on material A is inversely proportional to the thickness of material A through the $1/N_a$ term. This comes about because the external and anisotropy energies scale with the number of layers of the material, but the interfacial coupling is independent of the number of layers. This effective 1/thickness behavior clearly is connected to the behavior seen in Fig. 6 where the frequency of the Fe film resonance decreases as the number of Fe layers is increased.

We may now write $\mathbf{h}^a$ and $\mathbf{h}^b$ in terms of an average field $\langle \mathbf{h} \rangle$. This is done using the definition $f_a \mathbf{h}^a + f_b \mathbf{h}^b = \langle \mathbf{h} \rangle$ where the filling factors f_a and f_b are given by the usual definitions $f_a = N_a/(N_a+N_b)$ and $f_b = N_b/(N_a+N_b)$. Similarly the average magnetization will be $f_a \mathbf{a} M_a + f_b \mathbf{b} M_b = \langle \mathbf{m} \rangle$. In addition, one needs the boundary conditions $h_y^a + 4\pi M_a a_y = h_y^b + 4\pi M_b b_y$ and $h_x^a = h_x^b = \langle h_x \rangle$. Using these relations we may write the equation of motion matrix in terms of the average fields:

$$\begin{pmatrix} \langle h_y \rangle \\ -\langle h_x \rangle \\ \langle h_y \rangle \\ -\langle h_x \rangle \end{pmatrix} = \begin{pmatrix} i\omega/\gamma & H_1 + f_b 4\pi M_a & 0 & -H_{e1} - f_b 4\pi M_a \\ -H_1 & i\omega/\gamma & H_{e1} & 0 \\ 0 & -H_{e2} - f_a 4\pi M_b & i\omega/\gamma & H_2 + f_a 4\pi M_b \\ H_{e2} & 0 & -H_2 & i\omega/\gamma \end{pmatrix} \begin{pmatrix} a_x \\ a_y \\ b_x \\ b_y \end{pmatrix}. \tag{12}$$

The equations can now be inverted to solve for the a's and b's in terms of the average driving fields. After some simple manipulations we can then straightforwardly find analytic, though lengthy, expressions for the permeability tensor elements. We obtain

$$\mu_1 = 1 + \frac{1}{D} \left[4\pi f_1 M_a (H_{e1} + H_2) \{ H_1 H_2 + 4\pi M_a (f_2 H_2 - f_1 H_{e1}) - H_{e1} H_{e2} \} \right.$$

$$+ 4\pi f_2 M_b (H_{e2} + H_1) \{ H_1 H_2 + 4\pi M_b (f_1 H_1 - f_2 H_{e2}) - H_{e1} H_{e2} \}$$

$$+ 16\pi^2 M_a M_b \{ f_1 H_{e1}((f_1 - f_2)H_1 - 2f_2 H_{e2}) + f_2 H_{e2}(f_2 - f_1)H_2 + (f_1^2 + f_2^2)H_1 H_2 \}$$

$$\left. + (4\pi f_1 M_a [H_{e1} - H_1 + 4\pi f_2(2M_b - M_a)] + 4\pi f_2 M_b (H_{e2} - H_2 - 4\pi f_1 M_b))(\omega/\gamma)^2 \right], \tag{13}$$

$$\mu_2 = 1 + \frac{1}{D} \left[4\pi f_1 M_a H_{e1} \{ 2[(\omega/\gamma)^2 + H_1 H_2 - H_{e1} H_{e2}] - H_1 H_{e1} - H_2 H_{e2} - 4\pi(H_{e1} M_a + H_{e2} M_b) \right.$$

$$\left. + 4\pi f_2 H_2 M_b [H_1^2 - (\omega/\gamma)^2] + 4\pi f_1 H_1 M_a [H_2^2 - (\omega/\gamma)^2] + 16\pi^2 H_1 H_2 M_a M_b \} \right], \tag{14}$$

and

$$\mu_t = \frac{\omega/\gamma}{D} \{ 4\pi f_1 M_a [H_{e1}(H_{e2} + 2H_1 + 2H_2 + 4\pi M_a) + H_2^2 + 4\pi M_b H_2]$$

$$+ 4\pi f_2 M_b [H_{e2}(H_{e1} + 4\pi M_b) + H_1^2 + 4\pi M_a H_1] - 4\pi(f_1 M_a + f_2 M_b)(\omega/\gamma)^2 \}. \tag{15}$$

In the above expressions D is the determinant of the matrix in Eq. (12). It is given by

$$D = (H_1 H_2 - H_{e1} H_{e2})[4\pi f_1 H_1 M_b + 4\pi f_2 H_2 M_a + H_1 H_2 - H_{e1} H_{e2} - 8\pi f_1 M_a H_{e1}]$$

$$- (\omega/\gamma)^2 [8\pi f_1 M_a H_{e1} + 2H_{e1} H_{e2} + H_1^2 + H_2^2 + 4\pi f_2 H_1 M_a + 4\pi f_1 H_2 M_b] + (\omega/\gamma)^4. \tag{16}$$
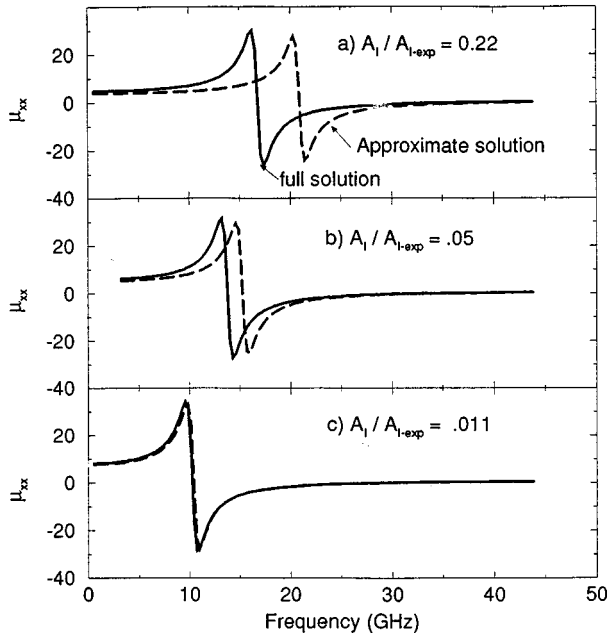
FIG. 8. Effective medium results compared to full theory for different values of the interfacial coupling. The structure is 36 layers of Fe/4 layers of Sm-Co. The solid lines show μ_{xx} for the full numerical calculation from Sec. II and the dashed lines show the results from the approximate calculation. The approximate calculation is good in the limit of weak interfacial coupling, as would be found in Fe/Cr/Fe type structures, but do not properly describe the strong coupling case of Fe/Sm-Co.

In Fig. 8 we compare the results of the analytical forms obtained above to the numerical results in the previous section for the μ_{xx} component of the permeability tensor. This figure is calculated for a 36 Fe layer/4 Sm-Co layer structure with $H = 2$ kG. In general, we see that the approximate method developed in this section does a good job of modeling the strength of the resonance. The position of the resonance is very accurate when the interfacial coupling is on the order of 1% of the bulk intrafilm coupling as is shown in Fig. 8(c). This would be appropriate for using these calculations for calculating the permeability of an Fe/Cr/Fe type structure where the interface coupling between the iron film is rather weak. In Fig. 8(c) we examine the case where the interfacial coupling is about 20% of the experimental value. In this case the position of the resonance is off by about 23%, although the shape is still quite good. Thus we conclude that for the strong coupling case one must use the full set of equations of motion as is done in Sec. II.

IV. APPLICATION TO A HIGH FREQUENCY FILTER

Several papers have recently suggested that high quality Fe films could be used as the active element in high frequency signal processing devices.[18–20] The coupled system Fe/Sm-Co discussed here has a significant advantage over Fe in that the operational frequency can be significantly increased without applying large external magnetic fields. Obviously, the properties of such a magnetically dependent device depend critically on the permeability tensor. It is
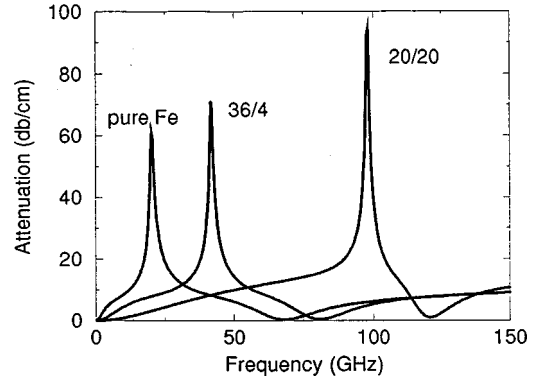

FIG. 9. Attenuation for waveguide structure as a function of frequency for different layered magnetic structures. The thickness of the GaAs layer is 10 μm, the thickness of the Fe/Sm-Co layer is 1 μm. The applied field is 2 kG with a Γ of 200 G.

therefore of interest to see if the permeability of the coupled system discussed here can still produce useful results.

We consider a planar waveguide structure consisting of a lower film of a highly conducting metal, then a dielectric film of GaAs, then the magnetic layered structure composed of Fe and Sm-Co and finally an upper film which is again a highly conducting metal. We can find the electromagnetic modes which propagate in this structure by solving Maxwell's equations in each region and applying the boundary conditions at the interfaces of the different films. The magnetic field is applied parallel to the long axis of the waveguide.

In our calculations[18,20] we focus on the attenuation of the electromagnetic wave due to the interaction with the magnetic material. The results for different structures are plotted in Fig. 9. The curve labelled ''pure Fe'' is for an Fe film 1 micron thick. We see two significant features, a peak in attenuation near 20 GHz and a dip in attenuation near 67 GHz. The attenuation peak could be used in making a notch filter which excludes certain frequencies from propagation. Similarly the dip in attenuation is useful in making a band pass filter. The remaining curves in Fig. 9 show the attenuation for 1 micron thick multilayers of Fe/Sm-Co with different layering patterns. As the amount of Sm-Co is increased and the amount of Fe is reduced, the frequency for both the peak and the dip shift substantially. This is to be expected from the results in the previous sections. Furthermore, the strength of the features, both peak and dip, are not substantially changed even when the layering includes 50% of Sm-Co. This indicates that these exchange-spring type layered structures may be very useful in high frequency signal processing applications.

V. SUMMARY AND CONCLUSIONS

We have investigated the frequency dependent magnetic permeability for a layered structure of Fe exchange coupled to a high anisotropy material of Sm-Co. We find that the coupled structure can have resonance frequencies which are shifted well above that for a simple Fe film. The shift in frequency depends on the interface coupling, the anisotropy of each material and the number of layers for each material.

We treat this problem through a numerical scheme initially and then find analytic solutions in the case of weak interfacial coupling. We find that the shift in resonance frequency decreases as the number of Fe layers is increased. In contrast, the frequency initially increases as the number of Sm-Co layers is increased, but levels off when the number of Sm-Co layers is close to the number of Fe layers.

We note that the true structure of Sm-Co is likely to be somewhat more complicated than that portrayed in our model. For example, the different atomic radii of Sm and Co favor compounds which can have alternating Co and Sm-Co layers.[21] Furthermore, the roughness for a thin film can be quite substantial; a rms roughness of 35 Å for a 160 Å film was reported.[22] In contrast, the characteristic lateral size is still quite large, on the order of 1000 Å and this supports our long wavelength approximation. Nonetheless the good agreement between the theoretical model and the experiment for both the static[1] and dynamic results argues that this model has reasonable validity.

The strength of the resonance measures the ability of the magnetic material to interact with electromagnetic waves. Our results show that the resonance strength of the coupled system is somewhat reduced from that of pure Fe, but that the reductions are not large. This is important for signal processing applications, and we illustrate this with a calculation for attenuation in a waveguide structure. Our calculations show that the Fe/Sm-Co layered structures produce results equivalent to those of pure Fe films, with the added feature that the operating frequency can be shifted upward substantially.

[1] E. E. Fullerton, J. S. Jiang, M. Grimsditch, C. H. Sowers, and S. D. Bader (unpublished); J. S. Jiang, E. E. Fullerton, M. Grimsditch, C. H. Sowers, and S. D. Bader, J. Appl. Phys. **83**, 6238 (1998).

[2] J. M. D. Coey, Solid State Commun. **102**, 101 (1977).

[3] R. Skomski, Phys. Rev. B **48**, 15 812 (1993).

[4] E. F. Kneller and R. Hawig, IEEE Trans. Magn. **27**, 3588 (1991).

[5] N. Raj and D. R. Tilley, Phys. Rev. B **36**, 7003 (1987).

[6] N. S. Almeida and D. L. Mills, Phys. Rev. B **38**, 6698 (1988).

[7] P. Grünberg, R. Schreiber, Y. Pang, M. B. Brodsky, and H. Sowers, Phys. Rev. Lett. **57**, 2442 (1986).

[8] B. Heinrich, Z. Celinski, J. F. Cochran, A. S. Arrott, K. Myrtle, and S. T. Purcell, Phys. Rev. B **47**, 5077 (1993).

[9] J. Unguris, R. J. Celotta, and D. T. Pierce, Phys. Rev. Lett. **67**, 140 (1991).

[10] S. S. P. Parkin, Phys. Rev. Lett. **67**, 3598 (1991).

[11] R. L. Stamps and R. E. Camley, Phys. Rev. B **54**, 15 200 (1996).

[12] R. Skomski and J. M. D. Coey, Phys. Rev. B **48**, 15 812 (1993).

[13] M. Vohl, J. Barnas, and P. Grünberg, Phys. Rev. B **39**, 12 003 (1989).

[14] B. Heinrich, in *Ultrathin Magnetic Structures II*, edited by B. Heinrich and J. A. C. Bland (Springer-Verlag, New York, 1994), pp. 195–290.

[15] R. L. Stamps, Phys. Rev. B **49**, 339 (1994).

[16] J. J. Krebs, P. Lubitz, A. Chaiken, and G. A. Prinz, Phys. Rev. Lett. **63**, 1645 (1989).

[17] R. L. Stamps, R. E. Camley, and R. J. Hicken, Phys. Rev. B **54**, 4159 (1996).

[18] E. Schloemann, R. Tutison, J. Weissman, H. J. Van Hook, and T. Vatimos, J. Appl. Phys. **63**, 3140 (1988).

[19] O. Archer, P. M. Jacquart, J. M. Fontaine, P. Baclet, and G. Perrin, IEEE Trans. Magn. **30**, 4533 (1994).

[20] R. E. Camley and D. L. Mills, J. Appl. Phys. **82**, 3058 (1997).

[21] See *Rare-earth Iron Permanent Magnets*, edited by J. M. D. Coey (Oxford University Press, New York, 1996).

[22] E. E. Fullerton, C. H. Sowers, J. E. Pearson, S. D. Bader, J. B. Patel, X. Z. Wu, and D. Lederman, J. Appl. Phys. **81**, 5637 (1997).